

Transmission Dynamics of COVID-19 Pandemic Non-pharmaceutical Interventions and Vaccination *

Bin-Guo WANG ^{†,1}, Shunxiang HUANG^{‡,§2}, Yongping XIONG ¹, Ming-Zhen XIN
¹, Jing LI², Jiangqian ZHANG¹, and Zhihui Ma¹

¹*School of Mathematics and Statistics, Lanzhou University, Lanzhou, Gansu 730000, China*

²*Institute of NBC Defense of PLA, Beijing 102205, China*

Abstract

Non-pharmaceutical interventions (NPIs) play an important role in the early stage control of COVID-19 pandemic. Vaccination is considered to be the inevitable course to stop the spread of SARS-CoV-2. Based on the mechanism, a SVEIR COVID-19 model with vaccination and NPIs is proposed. By means of the basic reproduction number R_0 , it is shown that the disease-free equilibrium is globally attractive if $\mathcal{R}_0 < 1$, and COVID-19 is uniform persistence if $\mathcal{R}_0 > 1$. Taking Indian dates for example in the numerical simulation, we find that our dynamical results fits well with the statistical dates. Consequently, we forecast the spreading trend of COVID-19 pandemic in India. Furthermore, our results imply that improving the intensity of NPIs will greatly reduce the number of confirmed cases. Especially, NPIs are indispensable even if all the people were vaccinated when the efficiency of vaccine is relatively low. By simulating the relationships of the basic reproduction number \mathcal{R}_0 , the vaccination rate and the efficiency of vaccine, we find that it is impossible to achieve the herd immunity without NPIs when the efficiency of vaccine is lower than 76.9%. Therefore, the herd immunity area is defined by the evolution of relationships between the vaccination rate and the efficiency of vaccine. In the study of two patchy, we give the conditions for India and China to be open to navigation. Furthermore, an appropriate dispersal of population between India and China is obtained. A discussion completes the paper.

Keywords: COVID-19; SARS; Reproduction numbers; Vaccination; NPIs;

AMS Subject Classification (2010): 34D20; 37B55; 92D30

*Supported by NSF of China 11501269 and 11731005.

[†]E-mail address:wangbinguo@lzu.edu.cn

[‡]E-mail address:huangshunxiang@mail.iap.ac.cn

[§]Contributed equally to this article

1 Introduction

Coronavirus disease 2019 (COVID-19), caused by a novel virus of the coronavirus genus (SARS-CoV-2), has been spreading globally. As of 28 June, 2021, there have been 180,817,269 confirmed cases of COVID-19, including 3,923,238 deaths [44]. The ongoing COVID-19 pandemic has caused a Once-in-a-Century global crisis [45]. Despite scientists worldwide racing to develop antiviral drugs, curative treatments are unavailable at the time of writing. the global economy is experiencing the worst plunge in recent history amid fears of further deterioration of the COVID-19 situation [11].

Non-pharmaceutical interventions (NPIs) such as quarantine, isolation, and social distancing play an important role in the control of SARS-CoV-2. Since the outbreak of COVID-19 was first detected in December 2019 in Wuhan, China [20], many authors have discussed the effects of various measures on the control of COVID-19 pandemic. For example, Tian et al. [32] suggested that the Wuhan travel ban or the national emergency response would have decreased to 744,000 ($\pm 156,000$) confirmed COVID-19 cases outside Wuhan. Since the airborne transmission by droplets and aerosols is important for the spread of viruses, face masks are a well-established preventive measure. Cheng et al. [6] found that most environments and contacts are under conditions of low virus abundance (virus-limited) where surgical masks are effective at preventing virus spread. More advanced masks and other protective equipments are required in potentially virus-rich indoor environments including medical centers and hospitals. Hu et al. [12] based on individual records of 1178 potential SARS-CoV-2 infectors and their 15,648 contacts in Hunan, China. Their results showed that SARS-CoV-2 susceptibility to infection increases with age, while transmissibility is not significantly different between age groups and between symptomatic and asymptomatic individuals. Contacts in households and exposure to first-generation cases are associated with higher odds of transmission. Considered the infectivity of individuals with, and susceptibility to, SARS-CoV-2 infection differs by age, schools were closed in the early months of the pandemic in most countries [34, 43], so that the low proportion of cases notified in young individuals [28] could be attributed to a low probability of developing symptoms [23, 24], a low susceptibility to infection [14, 36, 38], and/or few contact opportunities relative to other age groups. Senapati et al. [29] investigate that higher intervention effort is required to control the disease outbreak within a shorter period of time in India.

The transmission mechanism of SARS-CoV-2 makes it more difficult to fight against the disease. As far as the situation is concerned, vaccines are considered to be the most effective defense to control the disease completely. Various deployment strategies were being proposed to increase population immunity levels to SARS-CoV-2. In Saad-Roy et al. [30], the authors explored three scenarios of selection and found that a one-dose policy may increase the potential for antigenic evolution under certain conditions of partial population immunity. At same time, they highlighted the critical need to test viral loads and quantify immune responses after one vaccine dose, and to ramp up vaccination efforts throughout the world. In consideration of limited initial supply of SARS-CoV-2 vaccine, Bubar et al. [2] used a mathematical model to compare five age-stratified prioritization strategies. Following some of the WHO-SAGE recommendations, Acuña-Zegarrea et al. formulated an optimal control problem with mixed constraints to describe vaccination schedules [1].

According to the transmission mechanism of COVID-19, combining NPIs and vaccines, the population is divided into the following categories: susceptible individuals (S), vaccinated individuals (V), exposed individuals (E), infectious individuals (I) and recovered/removed individuals (R). Hence, a SVEIR model for COVID-19 is proposed. The SEIR model and its updates were successful in predicting the SARS epidemic in 2003-2004 [4], the H1N1 influenza pandemic in 2009 [21], and the MERS epidemic in 2012-2015 [15]. Recent studies have tried to use the SEIR model to predict the spread of COVID-19 in China. Raed et al. (2020) found that there would be approximately 21,022 (95% CrI 11,090-33,490) total infections by February 22 in Wuhan [16], while Wu et al. estimated that there would be 75,815 COVID-19 cases (95% CrI 37,304-130,330) in Wuhan by January 25, 2020 [33].

The basic reproduction number (ratio) \mathcal{R}_0 is a crucial threshold parameter in the study of disease transmission. In epidemiology, it is defined as the expected number of secondary cases produced by a single (typical) infection in a completely susceptible population and is used to measure the infection potential of an infectious disease [7, 22]. At the beginning of the transmission of coronavirus, based on likelihood and model analysis, Tang et al. [31] revealed that the basic reproduction number may be as high as 6.47, which showed that COVID-19 is highly infectious. By means of the basic reproduction number, Bubar et al. [2] found a highly mitigated spread during vaccine rollout. Riley et al. [27] used a model of constant exponential growth and decay, and quantified this fall and rise in prevalence in terms of halving and doubling times and the basic reproduction number. Noting that an important quantity in epidemiological models, the basic reproduction number, Cuevas-Maraver et al. [5] discussed in the realm of the model what consequences different additional intervention measures would have had at the level of deaths and of cumulative infections.

In the face of vaccine dose shortages and logistical challenges, how to deploy the strategies of NPIs and vaccination to increase population immunity levels to SARS-CoV-2 have not been fully considered in most of the above published. Mathematical models and field observations show that population dispersal can exert strong pressure on many infectious diseases [10, 19, 35]. Therefore, we choose a spatially discrete environment consisting of n patches, where a patch may represent a country or a city, and population movements between patches. Based on the infection mechanism of SARS-CoV-2, a novel susceptible-asymptomatic-symptomatic-recovered model with NPIs and vaccination (SASR) model in a patchy environment is proposed in Section 2. On the basis of the existence of the disease-free equilibrium, the definition and computation formulae of the basic reproduction number \mathcal{R}_0 are established. Drawing support from the basic reproduction number, the extinction and uniform persistence are shown in Section 3. The numerical simulation results not only consider the intensity of the intervention, the vaccination rate and the efficiency of vaccine but also incorporate the relationship between them and the basic reproducing number so as to get the control strategy of COVID-19 in Section 4. A brief discussion completes the paper.

2 SASR Compartmental Model

A matrix M is said to be nonnegative if all entries of M are nonnegative. If all off-diagonal

entries of M are nonnegative, then we say M is cooperative.

A $n \times n$ matrix $A = (a_{ij})_{n \times n}$ is said to be irreducible if for every nonempty, proper subset I of the set $N = \{1, 2, \dots, n\}$, there is an $i \in I$ and $j \in J = N \setminus I$ such that $|a_{ij}| > 0$.

Let S_i be the number of susceptible individuals in patch i , V_i be the number of the vaccinated individuals, E_{1i} be the number of the exposed individuals who are not contagious in the early stages in patch i , E_{2i} be the number of the exposed individuals who can infect the susceptible in patch i , and I_{1i} be the number of the infectious individuals in patch i who are contagious, I_{2i} be the number of the infectious individuals in patch i who are not contagious, R_i be the number of recovery individuals in patch i , N_i be the total population in patch i , that is, $N_i = S_i + V_i + E_{1i} + E_{2i} + I_{1i} + I_{2i} + R_i$. Furthermore, we suppose that N_i is constant. The population growth process can be described as in Figure 1.

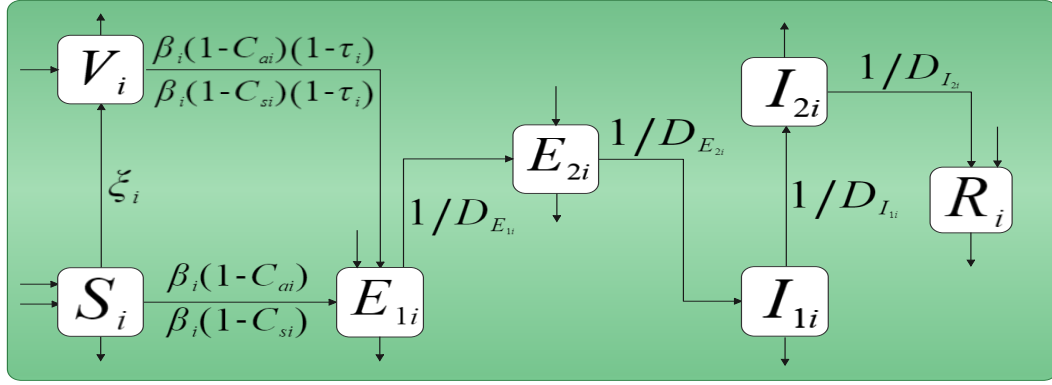


Figure 1: Compartmental diagram of COVID-19 transmission dynamics

The model is given by an autonomous system of ordinary differential equations

$$\begin{aligned}
\frac{dS_i}{dt} &= \Lambda_i - \beta_i(1 - C_{ai})\frac{S_i E_{2i}}{N_i} - \beta_i(1 - C_{si})\frac{S_i I_{1i}}{N_i} - \xi_i S_i - \mu_i S_i + \sum_{j=1}^n A_{ij} S_j, \\
\frac{dV_i}{dt} &= \xi_i S_i - \beta_i(1 - C_{ai})(1 - \tau_i)\frac{V_i E_{2i}}{N_i} - \beta_i(1 - C_{si})(1 - \tau_i)\frac{V_i I_{1i}}{N_i} - \mu_i V_i + \sum_{j=1}^n A_{ij} V_j, \\
\frac{dE_{1i}}{dt} &= \beta_i(1 - C_{ai})\frac{S_i E_{2i}}{N_i} + \beta_i(1 - C_{si})\frac{S_i I_{1i}}{N_i} + \beta_i(1 - C_{ai})(1 - \tau_i)\frac{V_i E_{2i}}{N_i} + \beta_i(1 - C_{si})(1 - \tau_i)\frac{V_i I_{1i}}{N_i} \\
&\quad - \frac{E_{1i}}{D_{E_{1i}}} - \mu_i E_{1i} + \sum_{j=1}^n B_{ij} E_{1j}, \\
\frac{dE_{2i}}{dt} &= \frac{E_{1i}}{D_{E_{1i}}} - \frac{E_{2i}}{D_{E_{2i}}} - \mu_i E_{2i} - d_i E_{2i} + \sum_{j=1}^n C_{ij} E_{2j}, \\
\frac{dI_{1i}}{dt} &= \frac{E_{2i}}{D_{E_{2i}}} - \frac{I_{1i}}{D_{I_{1i}}} - \mu_i I_{1i} - d_i I_{1i}, \\
\frac{dI_{2i}}{dt} &= \frac{I_{1i}}{D_{I_{1i}}} - \frac{I_{2i}}{D_{I_{2i}}} - \mu_i I_{2i}, \\
\frac{dR_i}{dt} &= \frac{I_{2i}}{D_{I_{2i}}} - \mu_i R_i + \sum_{j=1}^n D_{ij} R_j,
\end{aligned} \tag{2.1}$$

where Λ_i is the recruitment rate of susceptible class in patch i , C_{ai} and C_{si} denote the intensity of NPIs for incubation with infectiousness and infection with infectiousness individuals in patch i , respectively. β_i denotes the effective contact rate in patch i , ξ_i denotes the vaccination coverage

rate in patch i , μ_i is the natural death rate of the population in patch i , $D_{E_{1i}}$ and $D_{E_{2i}}$ are lengths of the incubation with non-infectiousness and incubation with infectiousness in patch i , respectively. $0 \leq \tau_i \leq 1$ denotes the vaccine efficacy in patch i ($\tau_i = 1$ represents a vaccine that offers 100% protection against infection, $\tau_i = 0$ models a vaccine that offers no protection at all). $D_{I_{1i}}$ and $D_{I_{2i}}$ are lengths of the infection with infectiousness and infection with non-infectiousness in patch i , respectively. d_i denotes the disease-induced mortality rate. A_{ij} stand for the dispersal rate from patch j to patch i of the susceptible and the vaccination. B_{ij} , C_{ij} and D_{ij} stand for the dispersal rates from patch j to patch i of the incubation with non-infectiousness, incubation with infectiousness, and recovery individuals, respectively. Biologically, we could suppose that the number of total human population in patch i stabilizes at $N_i > 0$.

Moreover, we assume

(A1) A_{ij}, B_{ij}, C_{ij} and D_{ij} are nonnegative constant, $\forall 1 \leq i \neq j \leq n$, and $[A_{ij}]_{n \times n}$, $[B_{ij}]_{n \times n}$, $[C_{ij}]_{n \times n}$ and $[D_{ij}]_{n \times n}$ are irreducible.

(A2) $\sum_{j=1}^n A_{ji} = \sum_{j=1}^n B_{ji} = \sum_{j=1}^n C_{ji} = \sum_{j=1}^n D_{ji} = 0$, $\forall i = 1, \dots, n$.

Note that (A1) assures that the immigration always occurs between two groups which are the arbitrary separation of n patches; (A2) means that deaths and births are neglected during the dispersal process.

For simplicity, set $\psi_t(x^0)$ be the solution of (2.1) with initial date $\psi_0(x^0) = x^0 \in \mathbb{R}_+^{7n}$. By [9, Theorem 2.1], we have the following.

Theorem 2.1 *For any $x^0 \in \mathbb{R}_+^{7n}$, system (2.1) has a unique nonnegative solution $\psi_t(x^0)$ with initial value $\psi_0(x^0) = x^0$, and all solutions are ultimately bounded and uniformly bounded.*

3 Basic Reproduction Number

In this section, we establish the definition and computation formulae of the basic reproduction number for system (2.1).

We first consider the disease-free solution of system (2.1). Let $E_{1i} = E_{2i} = I_{1i} = I_{2i} = 0$, $i = 1, \dots, n$, then we have

$$\begin{aligned} \frac{dS_i}{dt} &= \Lambda_i - \xi_i S_i - \mu_i S_i + \sum_{j=1}^n A_{ij} S_j, \\ \frac{dV_i}{dt} &= \xi_i S_i - \mu_i V_i + \sum_{j=1}^n A_{ij} V_j. \end{aligned} \tag{3.1}$$

By the similar arguments to those in [37], system (3.1) has a positive equilibrium $(S^*, V^*) = (S_1^*, S_2^*, \dots, S_n^*, V_1^*, V_2^*, \dots, V_n^*)$, which is globally attractive. Linearizing system (2.1) at the

disease-free equilibrium $(S^*, V^*, 0, 0, 0, 0)$, we get

$$\begin{aligned}
\frac{dE_{1i}}{dt} &= \beta_i(1 - C_{ai})\frac{S_i^*E_{2i}}{N_i} + \beta_i(1 - C_{si})\frac{S_i^*I_{1i}}{N_i} + \beta_i(1 - C_{ai})(1 - \tau_i)\frac{V_i^*E_{2i}}{N_i} + \beta_i(1 - C_{si})(1 - \tau_i)\frac{V_i^*I_{1i}}{N_i} \\
&\quad - \frac{E_{1i}}{D_{E_{1i}}} - \mu_i E_{1i} + \sum_{j=1}^n B_{ij}E_{1j}, \\
\frac{dE_{2i}}{dt} &= \frac{E_{1i}}{D_{E_{1i}}} - \frac{E_{2i}}{D_{E_{2i}}} - \mu_i E_{2i} - d_i E_{2i} + \sum_{j=1}^n C_{ij}E_{2j}, \\
\frac{dI_{1i}}{dt} &= \frac{E_{2i}}{D_{E_{2i}}} - \frac{I_{1i}}{D_{I_{1i}}} - \mu_i I_{1i} - d_i I_{1i}.
\end{aligned} \tag{3.2}$$

Define

$$F_1 = \begin{pmatrix} \beta_1(1 - C_{a1})\frac{S_1^*+(1-\tau_1)V_1^*}{N_1} & 0 & \cdots & 0 \\ 0 & \beta_2(1 - C_{a2})\frac{S_2^*+(1-\tau_2)V_2^*}{N_2} & \cdots & 0 \\ \vdots & \vdots & \ddots & \vdots \\ 0 & 0 & \cdots & \beta_n(1 - C_{an})\frac{S_n^*+(1-\tau_n)V_n^*}{N_n} \end{pmatrix},$$

$$F_2 = \begin{pmatrix} \beta_1(1 - C_{s1})\frac{S_1^*+(1-\tau_1)V_1^*}{N_1} & 0 & \cdots & 0 \\ 0 & \beta_2(1 - C_{s2})\frac{S_2^*+(1-\tau_2)V_2^*}{N_2} & \cdots & 0 \\ \vdots & \vdots & \ddots & \vdots \\ 0 & 0 & \cdots & \beta_n(1 - C_{sn})\frac{S_n^*+(1-\tau_n)V_n^*}{N_n} \end{pmatrix},$$

$$V_1 = \begin{pmatrix} \frac{1}{D_{E_{11}}} + \mu_1 - B_{11} & -B_{12} & \cdots & -B_{1n}(t) \\ -B_{21} & \frac{1}{D_{E_{12}}} + \mu_2 - B_{22} & \cdots & -B_{2n} \\ \vdots & \vdots & \ddots & \vdots \\ -B_{n1} & -B_{n2} & \cdots & \frac{1}{D_{E_{1n}}} + \mu_n - B_{nn} \end{pmatrix},$$

$$V_2 = \begin{pmatrix} \frac{1}{D_{E_{21}}} + \mu_1 + d_1 - C_{11} & -C_{12} & \cdots & -C_{1n} \\ -C_{21} & \frac{1}{D_{E_{22}}} + \mu_2 + d_2 - C_{22} & \cdots & -C_{2n} \\ \vdots & \vdots & \ddots & \vdots \\ -C_{n1} & -C_{n2} & \cdots & \frac{1}{D_{E_{2n}}} + \mu_n + d_n - C_{nn} \end{pmatrix},$$

$$V_3 = \text{diag}\left(\frac{1}{D_{I_{11}}} + \mu_1, \frac{1}{D_{I_{12}}} + \mu_2, \cdots, \frac{1}{D_{I_{1n}}} + \mu_n\right),$$

$$V_4 = \text{diag}\left(\frac{1}{D_{E_{11}}}, \frac{1}{D_{E_{12}}}, \cdots, \frac{1}{D_{E_{1n}}}\right)$$

and

$$V_5 = \text{diag}\left(\frac{1}{D_{E_{21}}}, \frac{1}{D_{E_{22}}}, \cdots, \frac{1}{D_{E_{2n}}}\right).$$

Let

$$Y = \begin{pmatrix} 0 & F_1 & F_2 \\ 0 & 0 & 0 \\ 0 & 0 & 0 \end{pmatrix}, Z = \begin{pmatrix} V_1 & 0 & 0 \\ -V_4 & V_2 & 0 \\ 0 & -V_5 & V_3 \end{pmatrix},$$

then (3.2) can be written by

$$\frac{du}{dt} = (Y - Z)u. \quad (3.3)$$

Motivated by the concept of next generation matrices introduced in [7, 22], we define the basic reproduction number of system (2.1) as

$$\mathcal{R}_0 := \rho(YZ^{-1}), \quad (3.4)$$

where $\rho(A)$ denotes the spectral radius of a matrix A .

Let $s(A)$ denotes the maximum real part of all the eigenvalues of the matrix A (the spectral abscissa of A). By a similar arguments to those in [7], we have the following statements.

Theorem 3.1 $\mathcal{R}_0 - 1$ has the same sign as $s(Y - Z)$.

The following two theorems give a threshold-type result on the extinction and uniform persistence of COVID-19 in terms of \mathcal{R}_0 .

Theorem 3.2 Assume (A1)-(A2) holds and $\mathcal{R}_0 < 1$, then the disease-free equilibrium $\mathcal{E}^* = (S^*, V^*, 0, 0, 0, 0, 0)$ of system (2.1) is globally attractive.

Proof. It is easy to see that $S(t)$ and $V(t)$ satisfy

$$\frac{dS_i}{dt} \leq \Lambda_i - \xi_i S_i - \mu_i S_i + \sum_{j=1}^n A_{ij} S_j$$

and

$$\frac{dV_i}{dt} \leq \xi_i S_i - \mu_i V_i + \sum_{j=1}^n A_{ij} V_j,$$

respectively. Since system (3.1) has a unique positive constant solution $(S_1^*, \dots, S_n^*, V_1^*, \dots, V_n^*)$, which is global asymptotically stable, by the comparison theorem, for any $x^0 \in \mathbb{R}_+^{7n}$ and $\varepsilon > 0$, there exists $t_0 > 0$ such that

$$S_i(t) \leq S_i^* + \varepsilon, V_i(t) \leq V_i^* + \varepsilon, \quad \forall t \geq t_0, \quad i = 1, \dots, n.$$

It then follows that

$$\begin{aligned} \frac{dE_{1i}}{dt} &\leq \beta_i(1 - C_{ai}) \frac{(S_i^* + \varepsilon)E_{2i}}{N_i} + \beta_i(1 - C_{si}) \frac{(S_i^* + \varepsilon)I_{1i}}{N_i} + \beta_i(1 - C_{ai})(1 - \tau_i) \frac{(V_i^* + \varepsilon)E_{2i}}{N_i} \\ &\quad + \beta_i(1 - C_{si})(1 - \tau_i) \frac{(V_i^* + \varepsilon)I_{1i}}{N_i} - \frac{E_{1i}}{D_{E_{1i}}} - \mu_i E_{1i} + \sum_{j=1}^n B_{ij} E_{1j}, \\ \frac{dE_{2i}}{dt} &\leq \frac{E_{1i}}{D_{E_{1i}}} - \frac{E_{2i}}{D_{E_{2i}}} - \mu_i E_{2i} + \sum_{j=1}^n C_{ij} E_{2j}, \\ \frac{dI_{1i}}{dt} &\leq \frac{E_{2i}}{D_{E_{2i}}} - \frac{I_{1i}}{D_{I_{1i}}} - \mu_i I_{1i}. \end{aligned}$$

we consider the following system

$$\begin{aligned} \frac{dE_{1i}}{dt} &= \beta_i(1 - C_{ai}) \frac{(S_i^* + \varepsilon)E_{2i}}{N_i} + \beta_i(1 - C_{si}) \frac{(S_i^* + \varepsilon)I_{1i}}{N_i} + \beta_i(1 - C_{ai})(1 - \tau_i) \frac{(V_i^* + \varepsilon)E_{2i}}{N_i} \\ &\quad + \beta_i(1 - C_{si})(1 - \tau_i) \frac{(V_i^* + \varepsilon)I_{1i}}{N_i} - \frac{E_{1i}}{D_{E_{1i}}} - \mu_i E_{1i} + \sum_{j=1}^n B_{ij} E_{1j}, \\ \frac{dE_{2i}}{dt} &= \frac{E_{1i}}{D_{E_{1i}}} - \frac{E_{2i}}{D_{E_{2i}}} - \mu_i E_{2i} + \sum_{j=1}^n C_{ij} E_{2j}, \\ \frac{dI_{1i}}{dt} &= \frac{E_{2i}}{D_{E_{2i}}} - \frac{I_{1i}}{D_{I_{1i}}} - \mu_i I_{1i}. \end{aligned} \quad (3.5)$$

Let $\lambda_i = \beta_i(1 - C_{ai})(\frac{(N_i^*+2\epsilon)-\tau_i(V_i^*+\epsilon)}{N_i})$ and $\eta_i = \beta_i(1 - C_{si})(\frac{(N_i^*+2\epsilon)-\tau_i(V_i^*+\epsilon)}{N_i})$, $i = 1, 2, \dots, n$.

Denote

$$F_1^\epsilon = \begin{pmatrix} \lambda_1 & 0 & \cdots & 0 \\ 0 & \lambda_2 & \cdots & 0 \\ \vdots & \vdots & \ddots & \vdots \\ 0 & 0 & \cdots & \lambda_n \end{pmatrix}, F_2^\epsilon = \begin{pmatrix} \eta_1 & 0 & \cdots & 0 \\ 0 & \eta_2 & \cdots & 0 \\ \vdots & \vdots & \ddots & \vdots \\ 0 & 0 & \cdots & \eta_n \end{pmatrix}.$$

Let

$$Y^\epsilon = \begin{pmatrix} 0 & F_1^\epsilon & F_2^\epsilon \\ 0 & 0 & 0 \\ 0 & 0 & 0 \end{pmatrix}.$$

Since $\mathcal{R}_0 < 1$, then $s(-Z + Y) < 0$. By the continuity of spectral bound, there exists a sufficiently small $\epsilon_1 > 0$ such that $s(-Z + Y^\epsilon) < 0$ for $0 < \epsilon < \epsilon_1$, which implies that the trivial solution of the system (3.5) is globally asymptotically stable. By the comparison theorem of ordinary differential equation, we deduce that $E_{1i} \rightarrow 0, E_{2i} \rightarrow 0, I_{1i} \rightarrow 0$ as $t \rightarrow \infty, \forall i = 1, 2, \dots, n$. It then follows that system (3.1) is the limiting system of S_i, V_i equation in system (2.1). We also could get that I_2, R equation admit the limiting system

$$\begin{aligned} \frac{dI_{2i}}{dt} &= -\frac{I_{2i}}{D_{I_{2i}}} - \mu_i I_{2i}, \\ \frac{dR_i}{dt} &= \frac{I_{2i}}{D_{I_{2i}}} - \mu_i R_i + \sum_{j=1}^n D_{ij} R_j. \end{aligned} \tag{3.6}$$

It is easy to see that the solutions in (3.6) convergence to $(0, \dots, 0, 0, \dots, 0)$. Finally, by the theory of asymptotically autonomous systems (see, e.g. [3]), we conclude that the solution of system (2.1) converges to $(S_1^*, \dots, S_n^*, V_1^*, \dots, V_n^*, 0, \dots, 0, 0, \dots, 0)$. This confirms the global attractivity of \mathcal{E}^* for system (2.1) under the condition $\mathcal{R}_0 < 1$, and hence completes the proof. \square

Theorem 3.3 *If $\mathcal{R}_0 > 1$, then there exists $\tilde{\epsilon} > 0$ such that the solution $(S(t), V(t), E_1(t), E_2(t), I_1(t), I_2(t), R(t))$ of system (2.1) with initial data x^0 in \mathbb{R}_+^{7n} and $(E_1(0), E_2(0), I_1(0)) > \hat{0}$ satisfies*

$$\liminf_{t \rightarrow \infty} E_{1i}(t) > \tilde{\epsilon}, \liminf_{t \rightarrow \infty} E_{2i}(t) > \tilde{\epsilon}, \liminf_{t \rightarrow \infty} I_{1i}(t) > \tilde{\epsilon}, \quad \forall i = 1, \dots, n.$$

Proof. Define

$$X = \mathbb{R}_+^{7n},$$

$$X_0 := \{(S, V, E_1, E_2, I_1, I_2, R) \in X : E_{1i} > 0, E_{2i} > 0, I_{1i} > 0, 1 \leq i \leq n\}$$

$$\partial X_0 := X \setminus X_0$$

Then X_0 and ∂X_0 are relatively open and closed in \mathbb{R}_+^{7n} , respectively. For any $x^0 \in X_0$, let $\psi_t(x^0)$ be the unique solution of system (2.1) with initial data x^0 . It is easy to see that X_0 is a positively invariant set. According to the arguments in Section 2, the solution of (2.1) is ultimately bounded

in X , which implies that $\psi_t : X \rightarrow X$ is point dissipative on X . It follows from [17, Theorem 3.4.8] that ψ_t has a global compact attractor \mathcal{A} .

Define

$$M_\partial := \{x^0 \in \partial X_0 : \psi_t(x^0) \in \partial X_0, \forall t \geq 0\}$$

and

$$\mathcal{M} := \{x^0 \in X : x_{1i}^0 = S_i^*, x_{2i}^0 = V_i^*, x_{3i}^0 = x_{4i}^0 = x_{5i}^0 = 0, \forall i = 1, \dots, n\}.$$

We now show that

$$M_\partial = \mathcal{M}.$$

For any $x^0 \in \mathcal{M}$, the solution $\psi_t(x^0)$ satisfies $E_{1i}(t, x^0) = 0, E_{2i}(t, x^0) = 0, I_{1i}(t, x^0) = 0, i = 1, \dots, n$ for all $t \geq 0$. Hence, $x^0 \in M_\partial$ and $\mathcal{M} \subset M_\partial$.

For any $x^0 \in \partial X_0 \setminus \mathcal{M}$, there is a i^* such that $(x_{3i^*}^0, x_{4i^*}^0, x_{5i^*}^0) = (E_{1i^*}(0), E_{2i^*}(0), I_{1i^*}(0)) > (0, 0, 0)$.

Case 1 Let $E_{1i^*}(0) > 0$. Since B_{ij} is cooperative, the third equation of system (2.1) satisfies

$$\frac{dE_{1i^*}}{dt} \geq -\frac{E_{1i^*}}{D_{E_{1i^*}}} - \mu_i E_{1i^*} + B_{i^*i^*} E_{1i^*}.$$

Furthermore, the fact that the matrix B_{ij} is irreducible implies that there exists a $t_0 > 0$ such that $E_{1i}(t) > 0$ for all $i = 1, \dots, n$ and $t \geq t_0$.

From the third equation of system (2.1), we can get $E_{2i}(t) > 0 \forall i = 1, \dots, n, t \geq t_0 + 1$. Then, from the fourth equation of system (2.1), we deduce that $I_{1i}(t) > 0$ for all $i = 1, \dots, n$ and $t \geq t_0 + 2$.

Case 2 Let $E_{2i^*}(0) > 0$. By the fourth equation of system (2.1), we have

$$\frac{dE_{2i^*}}{dt} \geq -\frac{E_{2i^*}}{D_{E_{2i^*}}} - \mu_i E_{2i^*} + C_{i^*i^*} E_{2i^*},$$

which is deduced from the fact that C_{ij} is cooperative. Thus, we can get $E_{2i^*}(t) > 0, \forall t > 0$. Now, the third equation satisfies

$$\frac{dE_{1i^*}}{dt} \geq \beta_{i^*}(1 - C_{ai^*}) \frac{S_{i^*} E_{2i^*}}{N_{i^*}} - \frac{E_{1i^*}}{D_{E_{1i^*}}} - \mu_i E_{1i^*} + B_{i^*i^*} E_{1i^*}.$$

It is easy to see that $E_{1i^*}(t) > 0$ for $t > 1$. By the arguments in **Case 1**, we can obtain that $(E_1(t), E_2(t), I_1(t)) \gg (0, \dots, 0, 0 \dots, 0, 0, \dots, 0)$ for all $t > t_0 + 3$.

Case 3 Let $I_{1i^*}(0) > 0$. By the fifth equation of system (2.1), we have

$$\frac{dI_{1i^*}}{dt} \geq -\frac{I_{1i^*}}{D_{I_{1i^*}}} - \mu_i I_{1i^*}.$$

Hence, we can get $I_{1i^*}(t) > 0, \forall t > 0$. Now, the second equation of system (2.1) satisfies

$$\frac{dE_{1i^*}}{dt} \geq \beta_{i^*}(1 - C_{si^*}) \frac{S_{i^*} I_{1i^*}}{N_{i^*}} - \frac{E_{1i^*}}{D_{E_{1i^*}}} - \mu_i E_{1i^*} + B_{i^*i^*} E_{1i^*}.$$

It is easy to see that $E_{1i^*}(t) > 0$ for $t > 1$. By the arguments in **Case 1**, we can obtain that $(E_1(t), E_2(t), I_1(t)) \gg (0, \dots, 0, 0 \dots, 0, 0, \dots, 0)$ for all $t > t_0 + 3$.

Then $M_\partial \subset \mathcal{M}$. Hence, $M_\partial = \mathcal{M}$.

We claim that $W^s(\mathcal{M}) \cap X_0 = \emptyset$, where $W^s(\mathcal{M})$ is the stable manifold of \mathcal{M} . Let $\bar{\lambda}_i = \beta_i(1 - C_{ai})\left(\frac{(N_i^* - 2\epsilon) - \tau_i(V_i^* - \epsilon)}{N_i}\right)$ and $\bar{\eta}_i = \beta_i(1 - C_{si})\left(\frac{(N_i^* - 2\epsilon) - \tau_i(V_i^* - \epsilon)}{N_i}\right)$, $\forall i = 1, 2, \dots, n$. Denote

$$\bar{F}_1^\epsilon = \begin{pmatrix} \bar{\lambda}_1 & 0 & \cdots & 0 \\ 0 & \bar{\lambda}_2 & \cdots & 0 \\ \vdots & \vdots & \ddots & \vdots \\ 0 & 0 & \cdots & \bar{\lambda}_n \end{pmatrix}, \bar{F}_2^\epsilon = \begin{pmatrix} \bar{\eta}_1 & 0 & \cdots & 0 \\ 0 & \bar{\eta}_2 & \cdots & 0 \\ \vdots & \vdots & \ddots & \vdots \\ 0 & 0 & \bar{\eta}_n & \end{pmatrix}.$$

Let

$$\bar{Y}^\epsilon = \begin{pmatrix} 0 & F_1^\epsilon & F_2^\epsilon \\ 0 & 0 & 0 \\ 0 & 0 & 0 \end{pmatrix}.$$

Since $\mathcal{R}_0 > 1$, then $s(Y - Z) > 0$. By the continuity of spectral bound, there exists a sufficiently small $\epsilon_1 > 0$ such that $s(\bar{Y}_\epsilon - Z) > 0$ for $0 < \epsilon \leq \epsilon_1$.

Claim. If $x^0 \in X_0$, then

$$\limsup_{t \rightarrow \infty} d(\psi_t(x^0), \mathcal{M}) \geq \epsilon_1$$

On the contrary, we assume that there exists $\bar{x}^0 \in X_0$ such that $\limsup_{t \rightarrow \infty} d(\psi_t(\bar{x}^0), \mathcal{M}) < \epsilon_1$. It then follows that there exists $t_0 > 0$ such that

$$S_i^* - \epsilon_1 < S_i(t) < S_i^* + \epsilon_1, V_i^* - \epsilon_1 < V_i(t) < V_i^* + \epsilon_1$$

for all $t \geq t_0$ and $i = 1, \dots, n$. Hence, we have

$$\begin{aligned} \frac{dE_{1i}}{dt} &\geq \beta_i(1 - C_{ai})\frac{(S_i^* - \epsilon_1)E_{2i}}{N_i} + \beta_i(1 - C_{si})\frac{(S_i^* - \epsilon_1)I_{1i}}{N_i} + \beta_i(1 - C_{ai})(1 - \tau_i)\frac{(V_i^* - \epsilon_1)E_{2i}}{N_i} \\ &\quad + \beta_i(1 - C_{si})(1 - \tau_i)\frac{(V_i^* - \epsilon_1)I_{1i}}{N_i} - \frac{E_{1i}}{D_{E_{1i}}} - \mu_i E_{1i} + \sum_{j=1}^n B_{ij}E_{1j}, \\ \frac{dE_{2i}}{dt} &\geq \frac{E_{1i}}{D_{E_{1i}}} - \frac{E_{2i}}{D_{E_{2i}}} - \mu_i E_{2i} + \sum_{j=1}^n C_{ij}E_{2j}, \\ \frac{dI_{1i}}{dt} &\geq \frac{E_{2i}}{D_{E_{2i}}} - \frac{I_{1i}}{D_{I_{1i}}} - \mu_i I_{1i}. \end{aligned} \tag{3.7}$$

Since $-Z + \bar{Y}_\epsilon$ is irreducible and essentially nonnegative, it has a positive eigenvector associated with $s(-Z + \bar{Y}_\epsilon) > 0$. By the comparison theorem of ordinary differential equations, we have $\lim_{t \rightarrow \infty} E_{1i}(t) = \infty$, $\lim_{t \rightarrow \infty} E_{2i}(t) = \infty$, $\lim_{t \rightarrow \infty} I_{1i}(t) = \infty$, a contradiction. The claim is proved.

The set $M_\partial = \mathcal{M}$ is an isolated invariant set and acyclic. By [26, Theorem 4.6], we conclude that system (2.1) is uniformly persistent in X_0 whenever $\mathcal{R}_0 > 1$. That is, there is a $\tilde{\epsilon} > 0$ such that

$$\liminf_{t \rightarrow \infty} E_{1i}(t) > \tilde{\epsilon}, \liminf_{t \rightarrow \infty} E_{2i}(t) > \tilde{\epsilon}, \liminf_{t \rightarrow \infty} I_{1i}(t) > \tilde{\epsilon}, \forall i = 1, \dots, n.$$

This completes the proof. \square

Remark 3.4 System (2.1) considers the dynamics of COVID-19 model with NPIs and vaccination. If we take $\tau_i = 0$ in the above discussion, then system (2.1) implies that NPIs for incubation with infectiousness and infection with infectiousness individuals is the only measure. Similarly, let $C_{si} = 0$ and $C_{ai} = 0$ in the above discussion, system (2.1) implies that the vaccination is considered only.

4 Numerical simulation

By the actual dates showed in [13], let $\beta_i = 0.7$, $D_{E_{1i}} = 2.9$ Day, $D_{E_{2i}} = 2.3$ Day, $D_{I_{1i}} = 2.9$ Day, $D_{I_{2i}} = 12$ Day, $\forall i = 1, 2, \dots, n$. In the case of one patchy, we take the data of India to estimate the roles of NPIs and vaccination in the prevention and controlling of COVID-19. In the case of two patchy, we give the conditions for India and China to be open to navigation. Furthermore, an appropriate dispersal of population between India and China is obtained.

4.1 The case of one patchy

Let $n = 1$ in system (2.1), it then follows from (3.4) that the basic reproduction number is

$$\mathcal{R}_0 = \frac{\beta_1 \Lambda_1 (\mu_1 + \xi_1 (1 - \tau_1)) (D_{E_{21}} (\mu_1 + \frac{1}{D_{I_{11}}}) (1 - C_{a1}) + 1 - C_{s1})}{\mu_1 N_1 D_{E_{11}} D_{E_{21}} (\xi_1 + \mu_1) (\mu_1 + \frac{1}{D_{E_{11}}}) (\mu_1 + \frac{1}{D_{I_{11}}}) (d_1 + \mu_1 + \frac{1}{D_{E_{21}}})}. \quad (4.1)$$

We estimate $d_1 = 0.00013$ Day⁻¹. According to the dates in [47, 48], we take $N_1 = 1380004000$, $\mu_1 = 0.00004$ Day⁻¹ and $\Lambda_1 = 65786$ People/Day. It follows from the references [39–41] that the vaccine efficacy of Pfizer-BioNTech COVID-19 Vaccine, Moderna COVID-19 Vaccine and Janssen COVID-19 Vaccine are 95%, 94% and 66%, respectively. Hence, we get the average efficacy of vaccine is 85%. The following is the cumulative and active cases of COVID-19 in India from April 1, 2021 to June 28, 2021 [46]. Take the average efficiency of vaccine $\tau_1 = 0.85$ and $\xi_1 = 0.05$ which is the date in Indian on April 1 [46]. Considering the existing prevention and control intensity, we assume that $C_{a1} = C_{s1} = 0.2$. According to the data of cumulative and active cases on April 1 in India, taking the initial value is $(S(0), V(0), E_1(0), E_2(0), I_1(0), I_2(0), R(0)) = (1297600506, 70104203, 129660, 102834, 115020, 475941, 11475836)$. Thus, the numerical simulation results are shown in Figure 2.

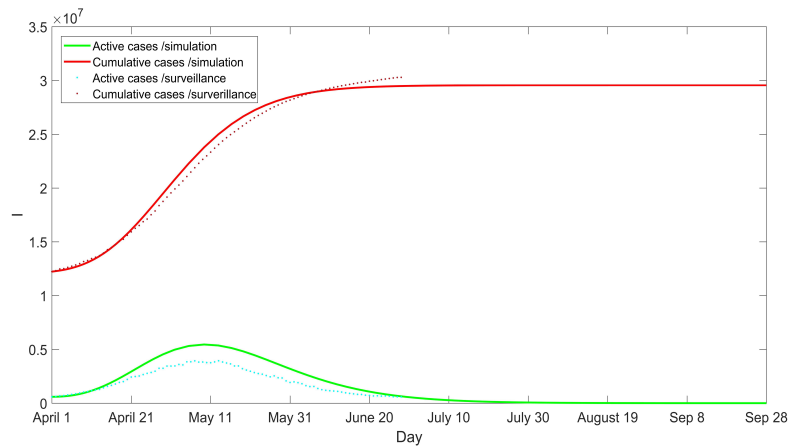


Figure 2: Numerical simulation of active and cumulative cases

The discrete points represent the real data of active and cumulative cases from April 1 to June 28, 2021 in India. We found that the dynamical results fit well with the statistical data(see Figure

2). If the existing protection intensity and vaccine injection schedule are maintained, the numerical simulation forecasts the trend of COVID-19 In India and the active cases will reach 100000 in July 25, 10000 in August 25 and 1000 in September 19.

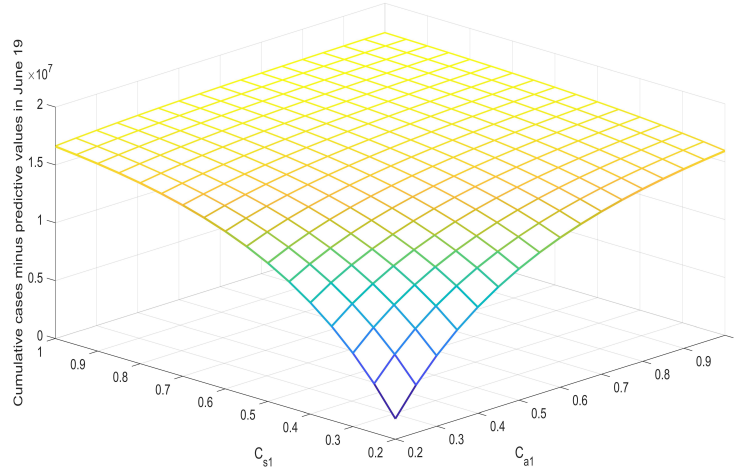


Figure 3: The decrement of numbers of infectious with the increase of C_{s1} and C_{a1} .

In the following, we investigate the role of NPIs in the controlling of COVID-19. Keeping other parameters unchanged, Figure 3 shows that C_{s1} and C_{a1} can effectively reduce the number of cumulative cases. Let P be the decrement of numbers of infectious with the increase of C_{s1} and C_{a1} . More intuitively, we have listed the specific numbers under the different intensity of NPIs(see Table 1).

Table 1: The relationship between P and C_{s1} and C_{a1}

$P \backslash C_{a1}$	0.2	0.25	0.3	0.35	0.4	0.45	0.5
C_{s1}							
0.2	1769611	4115444	6091986	7757921	9162980	10349134	11351706
0.25	4246751	6219307	7879821	9278475	10457744	11453237	12294780
0.3	6346002	8001037	9393367	10565718	11554108	12388618	13094313
0.35	8121646	9507596	10673095	11654365	12481781	13180634	13771950
0.4	9621232	10779821	11754026	12574353	13266301	13851057	14346209
0.45	10885953	11853052	12666328	13351389	13929545	14418491	14832893
0.5	11951462	12757688	13435882	14007466	14490192	14898792	15245468

It then follows from the dates in Table 1 if C_{s1} remains unchanged and C_{a1} is raised from 0.2 to 0.3, then there will be 6091986 fewer infected individual. Supposing that C_{a1} remains unchanged and C_{s1} is raised from 0.2 to 0.3, then there will be 6346002 fewer infected individual. If both C_{a1}

and C_{s1} are increased to 0.3, then there will be 9393367 fewer infected individual. According to the disease-induced mortality rate in Indian, if we take $C_{s1} = 0.2$, $C_{a1} = 0.3$, then 62566 people are saved; If $C_{s1} = 0.3$, $C_{a1} = 0.2$, then 65174 people are saved; If $C_{s1} = 0.3$ and $C_{a1} = 0.3$, then 96471 people are saved.

At present, the efficiency of vaccine is not relatively low. In the following, we assume that all people are vaccinated Janssen COVID-19 Vaccine and consider the relationship between \mathcal{R}_0 and C_{s1} , C_{a1} (see Figure 4).

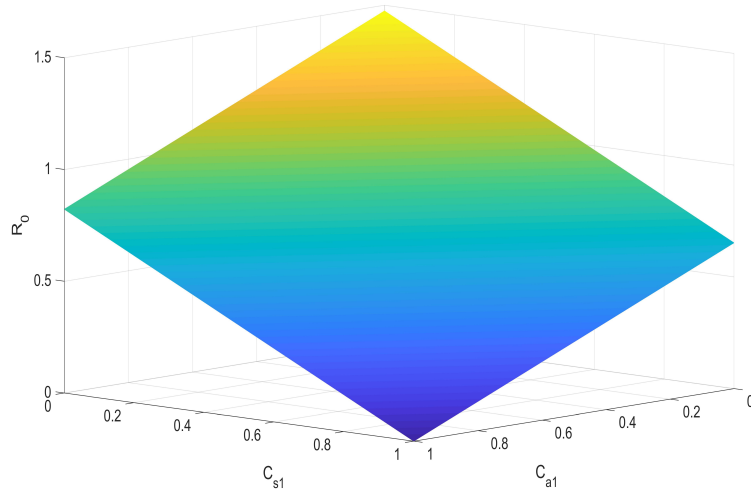


Figure 4: When $\tau_1 = 0.66$ and $\xi_1 = 1$, the image in three dimensions of relationship among \mathcal{R}_0 , C_{s1} and C_{a1} .

It can be seen from the above discussion that NPIs play a very significant role for the disease control. Figure 5 is the projection of Figure 4 on the $C_{s1} \times C_{a1}$ plane. The red and green area boundary line in Figure 5 represents $\mathcal{R}_0 = 1$. Figure 5 shows if (C_{a1}, C_{s1}) belongs to the green area, $\mathcal{R}_0 < 1$ while $\mathcal{R}_0 > 1$ in the red area. Our numerical results shows that NPIs are indispensable even if all the people were vaccinated when the efficiency of vaccine is relatively low. In other words, in order to control the spread of the disease, NPIs must be strengthened to make C_{s1} and C_{a1} in the green area A even if each people is vaccinated. In particular, we suggest that NPIs should be strengthened, not weakened in India.

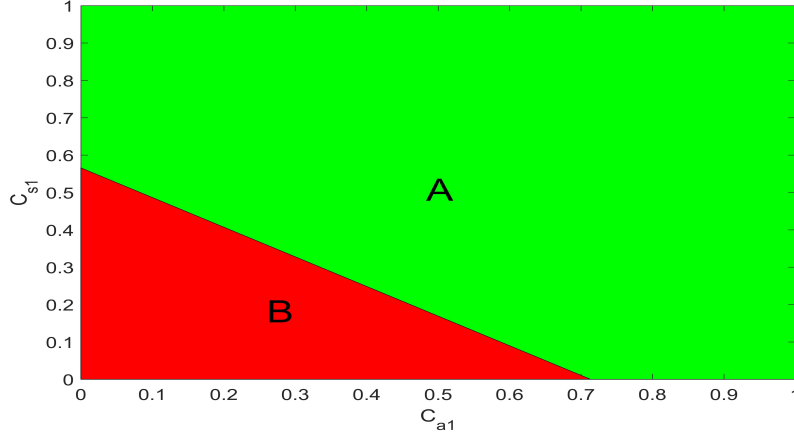


Figure 5: When $\tau_1 = 0.66$ and $\xi_1 = 1$, the relationship between C_{s1} and C_{a1} .

The herd immunity is our ultimate goal. In the following, we study the role of the vaccine in the absence of NPIs.

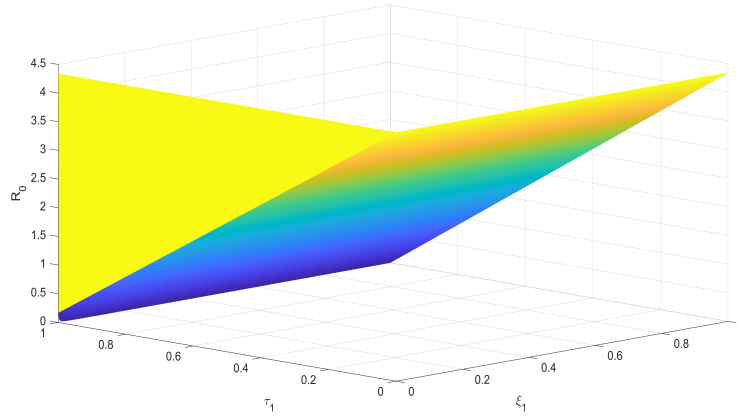


Figure 6: When $C_{s1} = 0$ and $C_{a1} = 0$, the relationship between ξ_1 and τ_1 and R_0 .

It then follows from Figure 6 that \mathcal{R}_0 decreases with the improvement of ξ_1 , and finally \mathcal{R}_0 is less than 1 when $\tau_1 = 0.95$. \mathcal{R}_0 is decreases and bigger than 1 even if $\xi_1 = 1$ when $\tau_1 = 0.66$. Let $\mathcal{R}_0 = 1$, $C_{a1} = C_{s1} = 0$ and $\xi_1 = 1$, it then follows from (4.1) that $\tau_1 = 0.769$. In other words, $\mathcal{R}_0 > 1$ always holds when $\tau_1 < 0.769$. Hence, we have gotten a minimum standard of the efficiency of vaccine.

In the face of vaccine dose shortages and logistical challenges, it's impossible for all people to be vaccinated in a shorten time. It is easy see that $\tau_1 \xi_1$ indicates the proportion of antibody produced after vaccination. Let $C_{a1} = C_{s1} = \xi_1 = \tau_1 = 0$, which implies that COVID-19 transmits without NPIs and vaccines. It then follows from (4.1) that $\mathcal{R}_0 = 4.3356$. Furthermore, we conclude if

$1 - \frac{1}{\mathcal{R}_0} < \tau_1 \xi_1$ is satisfied ([8]), then the herd immunity is formed.

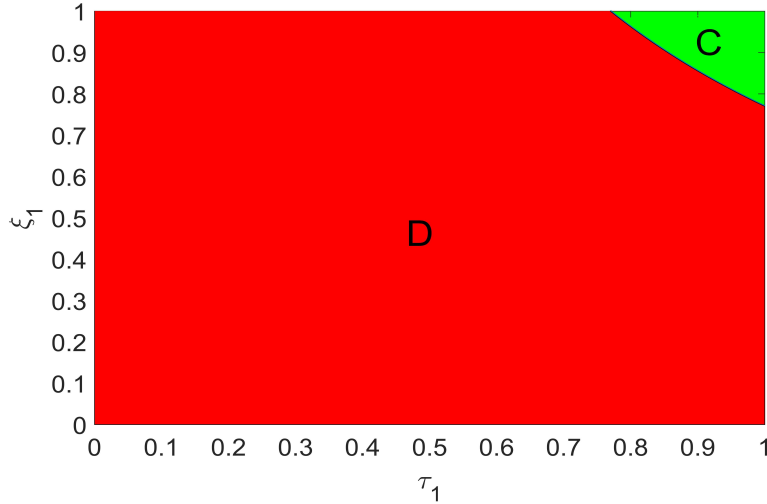


Figure 7: When $C_{a1} = 0$ and $C_{s1} = 0$, the relationship between herd immunity and τ_1 and ξ_1

From Figure 7, it reveals that $\xi_1 = 0.769$ when $\tau_1 = 1$, and $\tau_1 = 0.769$ if $\xi_1 = 1$. The intersection of the area C and D is called the herd immunity line which satisfies $\tau_1 \xi_1 = 0.769$ and C is the herd immunity area where the condition $\tau_1 \xi_1 > 0.769$ is satisfied.

4.2 The case of two patches

In this subsection, we take India and China for example and investigate the conditions for two countries to be open to navigation. Let $n = 1$ in system (2.1) to denote the case of India, while the case of China corresponds to $n = 2$. For simplicity, let

$$G = \begin{pmatrix} G_{11} & G_{12} \\ G_{21} & G_{22} \end{pmatrix} := \begin{pmatrix} \frac{1}{D_{E21}} + \mu_1 + d_1 - C_{11} & -C_{12} \\ -C_{21} & \frac{1}{D_{E22}} + \mu_2 + d_2 - C_{22} \end{pmatrix}^{-1} \begin{pmatrix} \frac{1}{D_{E21}} & 0 \\ 0 & \frac{1}{D_{E12}} \end{pmatrix} \times$$

$$\begin{pmatrix} \frac{1}{D_{E11}} + \mu_1 - B_{11} & -B_{12} \\ -B_{21} & \frac{1}{D_{E12}} + \mu_2 - B_{22} \end{pmatrix}^{-1}$$

$$H = \begin{pmatrix} H_1 & 0 \\ 0 & H_2 \end{pmatrix} := \begin{pmatrix} \frac{1}{D_{I11}} + \mu_1 & 0 \\ 0 & \frac{1}{D_{I12}} + \mu_2 \end{pmatrix}^{-1}$$

It then follows from (3.4) that

$$\begin{aligned}
\mathcal{R}_0 = & \frac{1}{2} \left((G_{11}\beta_1 \frac{S_1^* + (1-\tau_1)V_1^*}{N_1} (C_{a1} - 1 + \frac{H_1}{D_{E_{21}}} (C_{s1} - 1)) - G_{22}\beta_2 \frac{S_2^* + (1-\tau_2)V_2^*}{N_2} \times \right. \\
& (C_{a2} - 1 + \frac{H_2}{D_{E_{22}}} (C_{s2} - 1)))^2 + 4G_{12}G_{21}\beta_1\beta_2 \frac{(S_1^* + (1-\tau_1)V_1^*)(S_2^* + (1-\tau_2)V_2^*)}{N_1N_2} \times \\
& (C_{a1} - 1 + \frac{H_1}{D_{E_{21}}} (C_{s1} - 1))(C_{a2} - 1 + \frac{H_2}{D_{E_{22}}} (C_{s2} - 1)))^{\frac{1}{2}} - \frac{1}{2}G_{11}\beta_1 \frac{S_1^* + (1-\tau_1)V_1^*}{N_1} \times \\
& \left. (C_{a1} - 1 + \frac{H_1}{D_{E_{21}}} (C_{s1} - 1)) - \frac{1}{2}G_{22}\beta_2 \frac{S_2^* + (1-\tau_2)V_2^*}{N_2} (C_{a2} - 1 + \frac{H_2}{D_{E_{22}}} (C_{s2} - 1)), \right) \quad (4.2)
\end{aligned}$$

where $(S_1^*, S_2^*, V_1^*, V_2^*)$ is the disease-free solution with

$$\begin{aligned}
S_1^* &= \frac{-\Lambda_1\xi_2 - \Lambda_1\mu_2 - A_{12}\Lambda_2 + A_{22}\Lambda_1}{A_{11}\xi_2 + A_{22}\xi_1 + A_{11}\mu_2 + A_{22}\mu_1 - \xi_2\mu_1 - \xi_1\mu_2 - \mu_1\mu_2 - \xi_1\xi_2}, \\
S_2^* &= \frac{-\Lambda_2\xi_1 - \Lambda_2\mu_1 - A_{11}\Lambda_2 + A_{21}\Lambda_1}{A_{11}\xi_2 + A_{22}\xi_1 + A_{11}\mu_2 + A_{22}\mu_1 - \xi_2\mu_1 - \xi_1\mu_2 - \mu_1\mu_2 - \xi_1\xi_2}, \\
V_1^* &= \frac{-A_{12}S_2^*\xi_2 + A_{22}S_1^*\xi_1 - S_1^*\xi_1\mu_2}{A_{11}\mu_2 + A_{22}\mu_1 - \mu_1\mu_2}, \\
V_2^* &= \frac{-A_{21}S_1^*\xi_1 + A_{11}S_2^*\xi_2 - S_2^*\xi_2\mu_1}{A_{11}\mu_2 + A_{22}\mu_1 - \mu_1\mu_2}.
\end{aligned}$$

First, we consider the conditions for free navigations. By the dates in [42], let $\Lambda_2 = 32954$ People/Day, $N_2 = 1411780000$ People, $\mu_2 = 0.000036$ Day⁻¹. We estimate the $d_2 = 0.00016$ Day⁻¹. According to the dates in [49], the efficacy of Sinopharm COVID-19 Vaccine is 0.73 and Tianjin CanSino COVID-19 Vaccine is 0.66. Take the average efficacy of vaccine is 0.70. We estimate that the number of people traveled from China to India is 250000 and from India to China is 1400000 annually. Thus, $A_{21} = 2.78 \times 10^{-6}$ Day⁻¹, $B_{21} = 2.78 \times 10^{-6}$ Day⁻¹, $C_{21} = 2.78 \times 10^{-6}$ Day⁻¹, $D_{21} = 2.78 \times 10^{-6}$ Day⁻¹, $A_{12} = 4.85 \times 10^{-7}$ Day⁻¹, $B_{12} = 4.85 \times 10^{-7}$ Day⁻¹, $C_{12} = 4.85 \times 10^{-7}$ Day⁻¹ and $D_{12} = 4.85 \times 10^{-7}$ Day⁻¹. In the situation of without NPIs and vaccines, i.e., the other parameters are defined as the above and $\tau = \tau_i = \xi = \xi_i = C_{ai} = C_{si} = 0$, $i = 1, 2$, it then follows from (4.2) that $\mathcal{R}_0 = 4.0843$. By the formula of the herd immunity $1 - \frac{1}{\mathcal{R}_0} < \tau\xi$, the relationships between τ and ξ are shown in the following (see Figure 8).

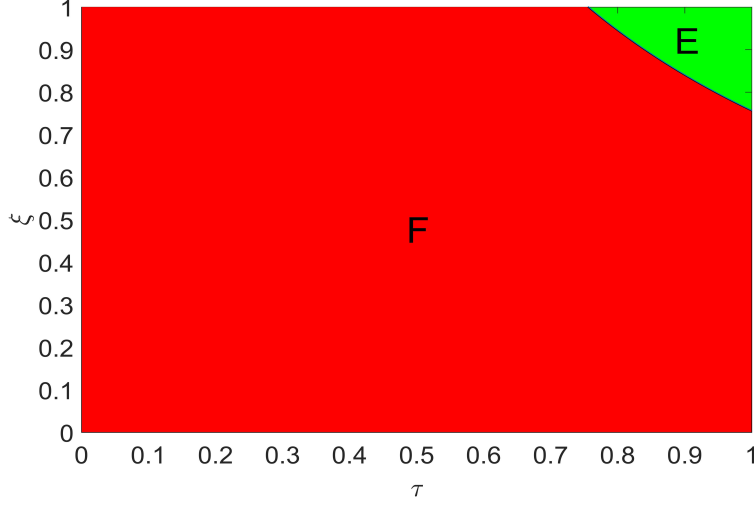


Figure 8: The relationship between herd immunity and ξ and τ .

It is easy to see from Figure 8 that $\xi = 0.755$ when $\tau = 1$, and $\tau = 0.755$ if $\xi = 1$. The area E is the herd immunity area. The above arguments imply that it is impossible to achieve the herd immunity since the average efficacy of vaccine $\tau = 0.70$. In other words, India and China do not meet the conditions for free navigations unless it is recommended to improve the efficiency of vaccinate or strengthen NPIs even if ξ reaches 100%.

In the following, we consider the influence of dispersal rate on the transmission of the disease. Let $C_{a1} = C_{s1} = 0.2$, $C_{a2} = C_{s2} = 0.6$, $\tau_1 = 0.85$, $\tau_2 = 0.7$, $\xi_1 = 0.23$, $\xi_2 = 0.82$ and assume $A_{21} = B_{21} = C_{21}$, $A_{12} = B_{12} = C_{12}$, the following is the relationship among A_{21} , A_{12} and \mathcal{R}_0 (see Figure 9).

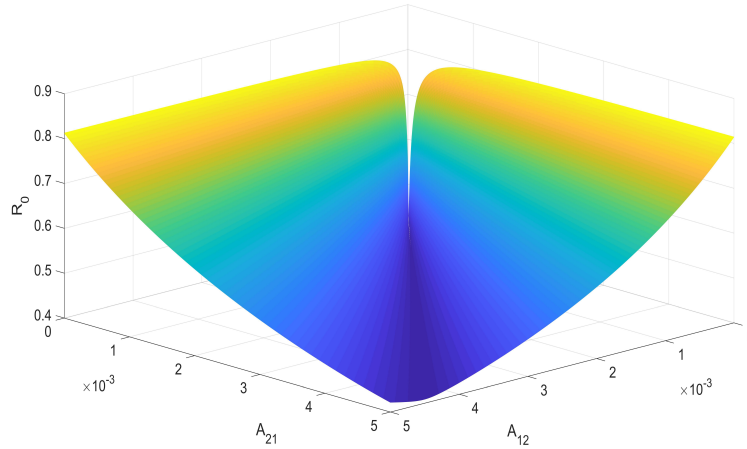


Figure 9: The relationships among A_{21} , A_{12} and \mathcal{R}_0 .

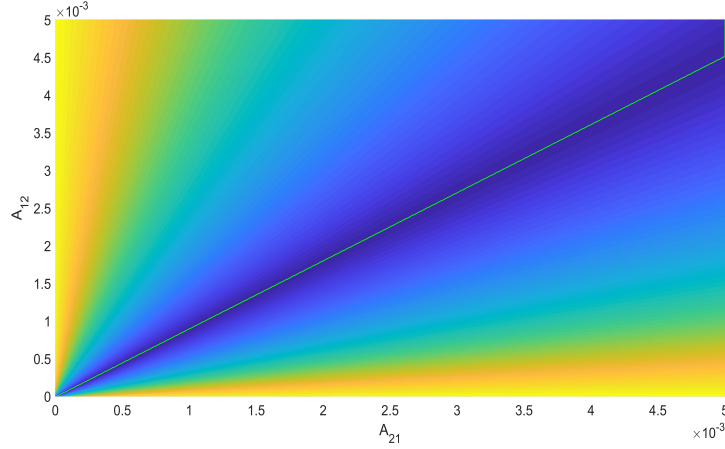


Figure 10: The projection of Figure 9.

Figure 10 implies that the basic reproduction number \mathcal{R}_0 may increase or decrease with the increase of dispersal rate. Let $A_{12} = A_{21} = 0$ and the other parameters be unchanged. It then follows from (4.1) that $\mathcal{R}_0 = 0.5208$ in India and $\mathcal{R}_0 = 0.2831$ in China. Let $A_{12} = 4.85 \times 10^{-7}$ and $A_{21} = 0$, then $\mathcal{R}_0 = 0.5247$. Let $A_{12} = 0$ and $A_{21} = 2.78 \times 10^{-6}$, then $\mathcal{R}_0 = 0.4870$. Let $A_{12} = 4.85 \times 10^{-7}$ and $A_{21} = 2.78 \times 10^{-6}$, then $\mathcal{R}_0 = 0.4910$. Fixed A_{21} , Figure 9 implies that there exists an A_{12} such that \mathcal{R}_0 takes the minimum value. The green line in Figure 10 is the set of all such points. Furthermore, we can ascertain that the smallest value $\mathcal{R}_0 = 0.04035$ which is corresponded by the point in the plane of $A_{12} = 2.8820 \times 10^{-9}$ and $A_{21} = 1.1636 \times 10^{-5}$ (see Figure 10). In other word, the appropriate dispersal of population of China to India is 1486 people, and the population of India to China is 5861071 people every year.

5 Discussion

Emphasizing non-pharmaceutical interventions(NPIs) and vaccines, the dynamics of a SVEIR COVID-19 model is considered by means of the basic reproduction number. In the case of one patchy, we considered the situations in India. Our numerical result predicts that the Indian epidemic will be controlled until October if the existing intensity of NPIs and vaccine injection schedule are maintained. If the outbreak occurs repeatedly, we suggest that NPIs should be strengthened. Furthermore, it is shown that NPIs are indispensable even if all the people were vaccinated when the efficiency of vaccine is relatively low. In order to obtain the herd immunity, we speculate in numerical simulation that the minimum standard of vaccine efficiency is 76.9%. In the face of vaccine dose shortages and logistical challenges, the herd immunity area is given. In the case of two patchy, we conclude that India and China do not meet the conditions for free navigation under nowadays situations. In order to prevent the disease outbreaks, the appropriate dispersal implies that people in the countries or regions with serious epidemic situation should be allowed to enter into the countries or regions where the epidemic situation is mild. Certainly, the

optimal strategy is that the counties affected slightly by COVID-19 supply medical supplies for the countries where COVID-19 is worst. We expect that COVID-19 will die out as soon as possible by the efforts of people of all over the world.

References

- [1] M. A. Acuña-Zegarrea et al., COVID-19 optimal vaccination policies: A modeling study on efficacy, natural and vaccine-induced immunity responses, *Mathematical Biosciences*, **337**(2021), 108614.
- [2] Bubar et al., Model-informed COVID-19 vaccine prioritization strategies by age and serostatus, *Science*, **371**(2021), 916–921.
- [3] C. Castillo-Chaves, H. R. Thieme, Asymptotically autonomous epidemic models. In: Arino O et al (eds) *Mathematical population dynamics: analysis of heterogeneity, I. Theory of epidemics*. Wuerz, Winnipeg, 33–50.
- [4] Gumel A. B., S. Ruan, T. Day et al. Modelling strategies for controlling SARS outbreaks. *Proceedings of the Royal Society of London Series B Biological Sciences*, **271**(2020), 2223–2232.
- [5] J.Cuevas-Maraver et al., Lockdown measures and their impact on single- and two-age-structured epidemic model for the COVID-19 outbreak in Mexico, *Mathematical Biosciences*, **336**(2021), 108590.
- [6] Y. Cheng et al., Face masks effectively limit the probability of SARS-CoV-2 transmission, *Science*, DOI:10.1126/science.abg6296, (2021).
- [7] P. van den Driessche, J. Watmough, Reproduction numbers and sub-threshold endemic equilibria for compartmental models of disease transmission, *Math Biosci*, **180**(2002), 29–48.
- [8] K. Dietz, Transmission and control of arbovirus diseases, D. Ludwig, K. L. Cooke, *Epidemiology, society for industrial and applied mathematics (SIAM)*, 1975, 104–121.
- [9] D. Gao, S. Ruan, An SIS patch model with variable transmission coefficients, *Math. Biosci.*, **232**(2011), 110–115.
- [10] D. Gao, S. Ruan, Malaria models with spatial effects, in *Analyzing and Modeling Spatial and Temporal Dynamics of Infectious Disease*, D. Chen, B. Moulin, and J. Wu, eds., John Wiley Sons., Hoboken, New Jersey, 2014, 111–138.
- [11] X. Gao et al., Crystal structure of SARS-CoV-2 Orf9b in complex with human TOM70 suggests unusual virus-host interactions, *Nature Communications* **12**(2021), 2843.
- [12] S. Hu et al. Infectivity, susceptibility, and risk factors associated with SARS-CoV-2 transmission under intensive contact tracing in Hunan, China, *Nature Communications*, **12**(2021), 1533.
- [13] S. Huang et al. Transmission Dynamics and High Infectiousness of Coronavirus Disease 2019, *Communications on Pure and Applied Analysis*, Submitted.
- [14] Q. Jing et al., Household secondary attack rate of COVID-19 and associated determinants in Guangzhou, China: a retrospective cohort study, *Lancet Infect. Dis.* **20**(2020), 1141–1150.
- [15] J. Lee, G. Chowell, E. Jung, A dynamic compartmental model for the Middle East respiratory syndrome outbreak in the Republic of Korea: A retrospective analysis on control interventions and superspreading events, *J. Theor. Biol.*, **408**(2016), 118–126.
- [16] J Read, J. Bridgen, D. Cummings et al. Novel coronavirus 2019-nCoV: early estimation of epidemiological parameters and epidemic predictions, 2020, DOI: org/10.1101/2020.01.2320018549.

- [17] J. K. Hale, Asymptotic behavior of dissipative systems. American Mathematical Society, Providence, 1988.
- [18] J. K. Hale, S. M. Verduyn Lunel, Introduction to Functional Differential Equations, Springer, New York, 1993.
- [19] X. Liu, P. Stechliniski, Transmission dynamics of a switched multi-city model with transport-related infections, *Nonlinear Anal. Real Word Appl.*, **14**(2013). 264–279.
- [20] Q. Li et al., Early transmission dynamics in Wuhan, China, of novel coronavirus-infected pneumonia, *N. Engl. J. Med.* **382**(2020), 1199–1207.
- [21] G. M. Hwang, P. J. Mahoney, J. H. James et al. A model-based tool to predict the propagation of infectious disease via airports, *Travel Medicine Infectious Disease*, **10**(2012), 32–42.
- [22] O. Diekmann, J. A. P. Heesterbeek, J. A. J. Metz, On the definition and the computation of the basic reproduction ratio R_0 in the models for infectious disease in heterogeneous populations, *J. Math. Biol.*, **28**(1990),365–382.
- [23] P. Poletti et al. Association of Age With Likelihood of Developing Symptoms and Critical Disease Among Close Contacts Exposed to Patients With Confirmed SARS-CoV-2 Infection in Italy. *JAMA Netw, Open* 4, e211085 (2021).
- [24] M. Pollán et al. Prevalence of SARS-CoV-2 in Spain (ENE-COVID): a nationwide, population-based seroepidemiological study, *Lancet* **396**(2020), 535–544.
- [25] H. L. Smith, Monotone dynamical system: an introduction to the theory of competitive and cooperative systems, American Mathematical society, Providence, 1995.
- [26] H, R, Thieme, Persistence under relaxed point-dissipativity (with application to an endemic model), *SIAM J Math Anal*, **24**(1993), 407–435.
- [27] Riley et al., Resurgence of SARS-CoV-2: Detection by community viral surveillance, *Science* **372**(2021), 990–995.
- [28] I. P. Sinha et al. COVID-19 infection in children, *Lancet Respir. Med.*, **8**(2020), 446–447.
- [29] A. Senapati, S. Rana , T. Das, J. Chattopadhyay, Impact of intervention on the spread of COVID-19 in India: A model based study, *Journal of Theoretical Biology*, **523**(2021), 110711.
- [30] C. M. Saad-Roy et al., Epidemiological and evolutionary considerations of SARS-CoV-2 vaccine dosing regimes, *Science*, DOI:10.1126/science.abg8663 (2021).
- [31] B. Tang et al., Estimation of the transmission risk of 2019-nCov and its implication for public health interventions, *Journal of Clinical Medicine*, 2020,9(2):462, DOI:10.3390/jcm9020462.
- [32] H. Tian et al., An investigation of transmission control measures during the first 50 days of the COVID-19 epidemic in China, *Science*, **368**(2020), 638–642.
- [33] J. T. Wu, K. Leung, G. M. Leung, Nowcasting and forecasting the potential domestic and international spread of the 2019-nCoV outbreak originating in Wuhan, China: a modelling study. *The Lancet*, **395**(2020), 689-697.
- [34] W. Van Lancker, Z. & Parolin, COVID-19, school closures, and child poverty: a social crisis in the making, *Lancet Public Health* 5, e243–e244 (2020).
- [35] W. Wang and X.Q. Zhao, An epidemic model in a patchy environment, *Math. Biosci.*, **190**(2004) 97–112.
- [36] J. Wu et al., Estimating clinical severity of COVID-19 from the transmission dynamics in Wuhan, China. *Nat. Med.* **26**(2020), 506–510.
- [37] B.-G. Wang , X.-Q. Zhao, Basic reproduction ratios for almost periodic compartmental epidemic models, *J Dyn Diff Equ*, **25**(2013), 535–562.
- [38] J. Zhang et al., Changes in contact patterns shape the dynamics of the COVID- 19 outbreak in China. *Science*, **368**(2020), 1481–1486.
- [39] CDC. The Pfizer-BioNTech COVID-19 Vaccine. <https://www.cdc.gov/coronavirus/2019-ncov/vaccines/different-vaccines/Pfizer-BioNTech.html>.

- [40] CDC. The Moderna COVID-19 Vaccine. <https://www.cdc.gov/coronavirus/2019-ncov/vaccines/different-vaccines/Moderna.html>.
- [41] CDC. The Janssen COVID-19 Vaccine. <https://www.cdc.gov/coronavirus/2019-ncov/vaccines/different-vaccines/janssen.html>.
- [42] NBS. The population data of 2020. <https://data.stats.gov.cn/easyquery.htm?cn=C01>.
- [43] United Nations Educational, Scientific and Cultural Organization. Education: from disruption to recovery. <https://en.unesco.org/covid19/educationresponse> (2020).
- [44] World Health Organization, WHO Coronavirus disease (COVID-19) Dashboard, URL: <https://covid19.who.int/> (Accessed 24 February 2021).
- [45] World Health Organization, WHO Coronavirus disease (COVID-19) Dashboard, URL: <https://covid19.who.int/> (2020).
- [46] <https://www.mygov.in/covid-19>.
- [47] <https://knoema.com/atlas/India/Population>.
- [48] <https://www.phb123.com/city/renkou/31223.html>.
- [49] <http://www.healthdata.org/covid/covid-19-vaccine-efficacy-summary>.